Modeling Human Multimodal Perception and Control Using Genetic Maximum Likelihood Estimation

P.M.T. Zaal,* D.M. Pool,†
Q.P. Chu,‡ M.M. van Paassen,§ M. Mulder¶ and J.A. Mulder‖
Delft University of Technology, Delft, The Netherlands

This paper presents a new method for estimating the parameters of multi-channel pilot models that is based on maximum likelihood estimation. To cope with the inherent nonlinearity of this optimization problem, the gradient-based Gauss-Newton algorithm commonly used to optimize the likelihood function in terms of output error is complemented with a genetic algorithm. This significantly increases the probability of finding the global optimum of the optimization problem. The genetic maximum likelihood method is successfully applied to data from a recent human-in-the-loop experiment. Accurate estimates of the pilot model parameters and the remnant characteristics were obtained. Multiple simulations with increasing levels of pilot remnant were performed, using the set of parameters found from the experimental data, to investigate how the accuracy of the parameter estimate is affected by increasing remnant. It is shown that only for very high levels of pilot remnant the bias in the parameter estimates

*Ph.D. student, Control and Simulation Division, Faculty of Aerospace Engineering, P.O. Box 5058, 2600GB Delft, The Netherlands; p.m.t.zaal@tudelft.nl. Student member AIAA.

†Ph.D. student, Control and Simulation Division, Faculty of Aerospace Engineering, P.O. Box 5058, 2600GB Delft, The Netherlands; d.m.pool@tudelft.nl. Student member AIAA.

‡Associate Professor, Control and Simulation Division, Faculty of Aerospace Engineering, P.O. Box 5058, 2600GB Delft, The Netherlands; q.p.chu@tudelft.nl. Member AIAA.

§Associate Professor, Control and Simulation Division, Faculty of Aerospace Engineering, P.O. Box 5058, 2600GB Delft, The Netherlands; m.m.vanpaassen@tudelft.nl. Member AIAA.

¶Associate Professor, Control and Simulation Division, Faculty of Aerospace Engineering, P.O. Box 5058, 2600GB Delft, The Netherlands; m.mulder@tudelft.nl. Member AIAA.

‖Professor, Control and Simulation Division, Faculty of Aerospace Engineering, P.O. Box 5058, 2600GB Delft, The Netherlands; j.a.mulder@tudelft.nl. Member AIAA.

is substantial. Some adjustments to the maximum likelihood method are proposed to reduce this bias.

Nomenclature

A	State matrix	
A_d	Disturbance sinusoid amplitude	deg
A_t	Target sinusoid amplitude	deg
B	Input matrix	
C	Output matrix	
D	Feedthrough matrix	
e	Tracking error signal	deg
f	Probability density function	-
f_d	Disturbance forcing function	deg
f_t	Target forcing function	deg
$H(s)$	Transfer function	
$H(j\omega)$	Frequency response function	
H_n	Remnant filter	
H_{nm}	Neuromuscular dynamics	
H_{pe}	Pilot visual response	
$H_{p\theta}$	Pilot motion response	
H_{sc}	Semicircular canal dynamics	
H_{θ,δ_e}	Controlled pitch dynamics	
j	Imaginary unit	-
L	Likelihood function	-
K_m	Motion perception gain	-
K_n	Remnant filter intensity	-
K_v	Visual perception gain	-
$K_{\delta_e,u}$	Pitch stick gain	-
$M_{\Theta\Theta}$	Fisher information matrix	
m	Number of samples	-
N	Remnant Fourier transform	-
N_e	Order of the error response state matrix	-
n	Pilot remnant signal	deg
n_d	Disturbance frequency integer factor	-
n_t	Target frequency integer factor	-
S	Spectrum	

s	Laplace variable	-
T_{lead}	Visual lead time constant	s
T_{lag}	Visual lag time constant	s
T_m	Measurement time	s
T_{sc_1}, T_{sc_2}	Semicircular canal time constants	s
t	Time	s
u	Pilot control signal	deg
$\bar{x}$	State vector	

Symbols

α	Line search parameter	-
δ_e	Elevator deflection	deg
ϵ	Prediction error	deg
ζ_n	Remnant filter damping	-
ζ_{nm}	Neuromuscular damping	-
Θ	Parameter vector	
θ	Pitch angle	deg
$\ddot{\theta}$	Pitch acceleration	deg s^{-2}
μ	Mean	
σ	Standard deviation	
τ_m	Motion perception time delay	s
τ_v	Visual perception time delay	s
ϕ	Sinusoid phase shift	rad
ω	Frequency	rad s^{-1}
ω_m	Measurement base frequency	rad s^{-1}
ω_n	Remnant filter break frequency	rad s^{-1}
ω_{nm}	Neuromuscular frequency	rad s^{-1}

Subscripts

e	pilot error response
d	disturbance
t	target
θ	pilot pitch response

I. Introduction

In manual control of aircraft, pilots combine information from cockpit instruments, their view of the outside world and physical motion sensations to achieve a suitable control action. Knowledge on how pilots use these different types of motion cues not only gives more insight into human motion perception processes, but it is also crucial to the design of manual control systems and the tuning of flight simulators.[1,2]

Many researchers applied multi-channel pilot models in their efforts to explain and quantify the effects of different modalities on pilot control behavior.[3–9] Human manual vehicle control behavior is an inherently nonlinear and time-varying closed-loop process. For carefully designed control tasks, however, the control behavior of well-trained individuals can be accurately described with quasi-linear pilot models.[10] Such models consist of a linear part that describes a pilot's response to all perceived variables in terms of control-theoretical elements, supplemented with a remnant signal that accounts for all nonlinear contributions to the observed control behavior. For tasks where pilots perceive information from multiple modalities – e.g., visual and motion – these linear pilot models generally have a multi-channel structure, where the response to the different modalities is separated. The characteristics of such linear pilot responses are defined by the model parameters, such as weighing gains and time delays. Values for these parameters, which can be determined from experimental data using mathematical identification techniques, help to explain the effects of different perceptual modalities on pilots' control behavior in control-theoretical terms.

Parameter estimation techniques currently employed to estimate the parameters of a multi-channel pilot model use either Fourier transforms[11] or linear time-invariant models[8] to obtain non-parametric pilot describing functions in the frequency domain. In a second step, the parameters of a multi-channel pilot model are then optimized to yield an optimal fit to these frequency responses. These methods have two main disadvantages. First, the accuracy of the parameter estimate is affected by biases that originate from *both* identification steps. In addition, for these identification methods to give accurate results, highly specific demands on the design of the control task – and specifically the adopted forcing functions – need to be met.[8]

An alternative to these frequency-domain parameter estimation methods are time-domain identification procedures, which allow for estimation of model parameters from time-domain data directly. For such time-domain identification techniques, the requirements to ensure the identifiability of a model are significantly less stringent.[12] Few studies are described in the literature that investigate the application of time-domain identification techniques to pilot modeling.[13–18] These studies only considered very simple pilot models and provide little detail of the identification procedure.

Maximum likelihood estimation is an example of a statistical time-domain identification method that, for instance, has been successfully applied to the identification of aircraft stability and control derivatives from flight test data[19–21] and of air- and spacecraft structural modes.[22,23] This study focuses on the application of a maximum likelihood parameter estimation algorithm to the problem of multi-channel pilot model identification. For the development of this algorithm, an output-error structure is assumed for the quasi-linear pilot model. Of particular interest are the steps that need to be taken to make the identification technique suitable for coping with the inherent nonlinearity and many local minima of the cost function. To cope with these nonlinearities and local minima, the maximum likelihood method is enhanced with a genetic algorithm. Data from a recent human-in-the-loop experiment,[2] which was performed in the SIMONA Research Simulator at Delft University of Technology, is used to test the genetic maximum likelihood algorithm. To evaluate the performance of this parameter estimation method with increasing levels of pilot remnant, the average bias and standard deviation of the parameter estimates are assessed using pilot model simulations.

The structure of the paper is as follows. First, the parameter estimation problem for multi-channel pilot models will be discussed. Then, the genetic maximum likelihood estimation procedure will be explained in detail and parameter estimation results from experimental data will be given. The paper ends with a discussion and conclusions.

II. The Parameter Estimation Problem

A manual vehicle control task that was investigated in a recent human-in-the-loop experiment will be considered as an example of a typical multi-channel pilot model identification problem in this paper. The objective of the experiment was to investigate the effects of rotational and vertical motion during aircraft pitch attitude control in a disturbance-rejection task.[2] It was found that the presence of rotational pitch motion significantly affected pilot control behavior, making aircraft pitch attitude control a clear example of a multi-loop control task.

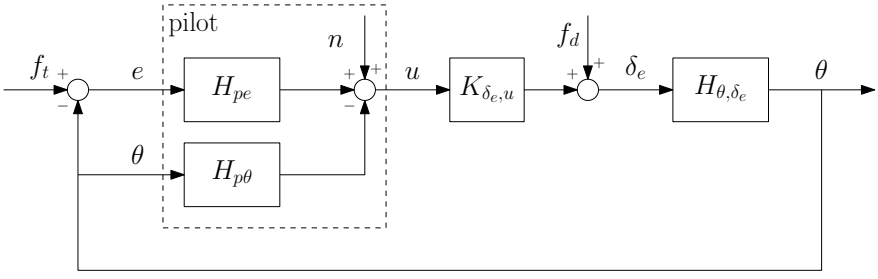

Figure 1. Multi-loop representation of a closed-loop aircraft pitch control task.

II.A. The Multi-Loop Control Task

In Figure 1, a schematic representation of the pitch attitude control task that is studied in this paper is depicted. As can be seen in this figure, the pilot acts as a feedback controller on the pitch dynamics of an aircraft, H_{θ,δ_e}. For this experiment, the controlled pitch dynamics were those of a Cessna Citation II aircraft as given by:

$$H_{\theta,\delta_e}(s) = -10.6189\frac{s+0.9906}{s(s^2+2.756s+7.612)}. \tag{1}$$

In addition to the tracking error e, which is the difference between the current and the desired pitch attitude as perceived from the compensatory visual display, information about the aircraft pitch attitude can be perceived via physical rotational motion. Hence, the total pilot response consists of the contributions of two linear response functions, H_{pe} and $H_{p\theta}$. A remnant signal n is added to the linear model output representing the nonlinear behavior. The gain $K_{\delta_e,u}$ in Figure 1 represents the scale factor between sidestick and elevator deflection. Two forcing functions, a disturbance f_d and target f_t, are used to excite the combined pilot-aircraft system. The target signal gives the desired pitch attitude; the disturbance signal can be considered as turbulence acting on the aircraft, perturbing the pitch angle.

II.B. The Multi-Channel Pilot Model

The linear response functions are parametrized by gains and time constants, the pilot equalization; time delays and neuromuscular dynamics, the pilot limitations; and vestibular dynamics, the pilot sensor dynamics. Based on McRuer's precision model[10] and Van der Vaart's multi-channel pilot model,[6] appropriate models for the linear response functions H_{pe} and $H_{p\theta}$ for control of the pitch dynamics defined by Eq. (1) are given by:[2]

$$H_{pe}(j\omega) = K_v\frac{(1+j\omega T_{lead})^2}{(1+j\omega T_{lag})}e^{-j\omega\tau_v}H_{nm}(j\omega), \tag{2}$$

and

$$H_{p\theta}(j\omega) = (j\omega)^2 H_{sc}(j\omega) K_m e^{-j\omega\tau_m}H_{nm}(j\omega). \tag{3}$$

In Eq. (2), which describes the response to visual motion cues, K_v is the visual perception gain, T_{lead} the visual lead time constant, T_{lag} the visual lag time constant and τ_v the visual perception time delay. Rotational pitch motion is mainly perceived with the semi-circular canals of the vestibular system, which are sensitive to pitch acceleration.[7] The model for the pitch motion perception channel $H_{p\theta}$ (Eq. (3)) therefore includes the dynamics of the

semi-circular canals H_{sc}, the motion perception gain K_m and a motion perception time delay τ_m.

As can be verified from the presence of H_{nm} in both Eq. (2) and Eq. (3), the total linear pilot response is attenuated by the dynamics of the neuromuscular system. The neuromuscular system is modeled as a second-order mass-spring-damper system, of which the damping ζ_{nm} and natural frequency ω_{nm} are parameters to be estimated:

$$H_{nm}(j\omega) = \frac{\omega_{nm}^2}{\omega_{nm}^2 + 2\zeta_{nm}\omega_{nm}j\omega + (j\omega)^2}. \tag{4}$$

Finally, the dynamics of the semi-circular canals, which are part of the pitch motion perception channel of the pilot model, are given by:

$$H_{sc}(j\omega) = \frac{1 + j\omega T_{sc_1}}{1 + j\omega T_{sc_2}}, \tag{5}$$

with $T_{sc_1} = 0.11$ and $T_{sc_2} = 5.9$ seconds. These values are taken from previous research[7] and are assumed fixed when modeling pilot control behavior for the pitch control task defined in Figure 1. The parameter vector Θ, with a total of eight parameters to be estimated, is given by:

$$\Theta = \left[K_v \;\; T_{lead} \;\; T_{lag} \;\; \tau_v \;\; K_m \;\; \tau_m \;\; \zeta_{nm} \;\; \omega_{nm}\right]^T. \tag{6}$$

II.C. Forcing Functions

For reliable identification of both the pilot visual and motion responses with previously used parameter estimation methods, two independent forcing function signals are required. For the control task described in Figure 1, both the target and disturbance forcing function signals (f_t and f_d) were defined as sums of ten sine waves with different frequencies, amplitudes and phase shifts:

$$f_t(t) = \sum_{k=1}^{10} A_t(k)\sin\left(\omega_t(k)t + \phi_t(k)\right), \tag{7}$$

$$f_d(t) = \sum_{k=1}^{10} A_d(k)\sin\left(\omega_d(k)t + \phi_d(k)\right). \tag{8}$$

To allow for use of spectral methods in the analysis of the experimental data, the forcing function sine wave frequencies were all defined as integer multiples of the experimental measurement time base frequency, $\omega_m = 2\pi/T_m$ with $T_m = 81.92$ seconds. The corresponding integer factors n_t and n_d are listed in Table 1, together with the target and disturbance

signal frequencies, amplitudes and phases.

Table 1. Multi-sine forcing function properties.

	disturbance, f_d				target, f_t			
k, –	n_d, –	ω_d, rad s^{-1}	A_d, deg	ϕ_d, rad	n_t, –	ω_t, rad s^{-1}	A_t, deg	ϕ_t, rad
1	5	0.383	0.344	-0.269	6	0.460	0.698	1.288
2	11	0.844	0.452	4.016	13	0.997	0.488	6.089
3	23	1.764	0.275	-0.806	27	2.071	0.220	5.507
4	37	2.838	0.180	4.938	41	3.145	0.119	1.734
5	51	3.912	0.190	5.442	53	4.065	0.080	2.019
6	71	5.446	0.235	2.274	73	5.599	0.049	0.441
7	101	7.747	0.315	1.636	103	7.900	0.031	5.175
8	137	10.508	0.432	2.973	139	10.661	0.023	3.415
9	171	13.116	0.568	3.429	194	14.880	0.018	1.066
10	226	17.334	0.848	3.486	229	17.564	0.016	3.479

The target signal was defined to have only a quarter of the power of the disturbance signal to make the task primarily a disturbance-rejection task.[2]

II.D. Parameter Estimation Methods

Estimation of multi-channel pilot model parameters from measurement data is a highly nonlinear optimization problem. First of all, a linear model is fit on data that is inherently nonlinear. The fact that the models are nonlinear in their parameters further increases the nonlinearity of the optimization problem. Due to these nonlinearities, the resulting cost function contains many local minima in addition to the global minimum.

In addition, it is apparent from the model structure given in Eq. (2) and Eq. (3) that the lead term in the visual perception channel and the lead resulting from the integrating action of the semicircular-canal dynamics in the vestibular channel are more or less interchangeable. If multiple terms in a model can cause the same overall response, the model is overdetermined, which adds to the number of local minima. It is found in previous research that the occurrence of these local minima is highly dependent on the controlled dynamics, the type of forcing function and even the subject who performed the experiment.[24]

Many different techniques can be applied to estimate the parameters of a multi-channel pilot model from measurement data. Figure 2 illustrates that two groups can be distinguished, parameter estimation in the frequency domain and parameter estimation in the time domain.

II.D.1. Frequency-Domain Techniques

Parameter estimation in the frequency domain requires an additional step, to transform the measured time-domain data to the frequency domain, as illustrated in Figure 2. In this additional step, Fourier coefficients (FC) or linear time-invariant (LTI) models (e.g.,

autoregressive exogeneous (ARX) models) are used to estimate non-parametric frequency response functions.[8,11] These non-parametric frequency responses are then used in a second step, in which a multi-channel pilot model is fit by adjusting its parameters. For estimating the pilot model parameters a frequency-domain criterion is used, which results in a nonlinear optimization problem.[8,9,25]

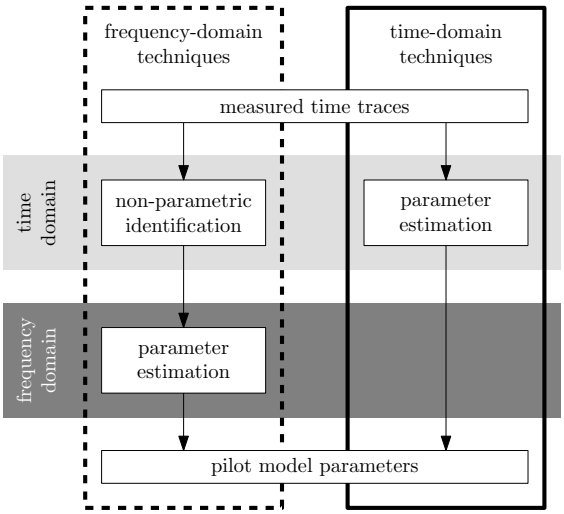

Figure 2. Comparison of pilot model parameter estimation methods.

With some exceptions, in the field of human operator modeling, parameter estimation has mainly been performed in the frequency domain.[3,4,6–9,11,25,26] An advantage of this technique is that the first step serves as a data reduction step, which makes the parameter optimization efficient in terms of computational power. Another advantage of this method is that the non-parametric frequency response functions provide an indication of the pilot model structure required for describing the pilot dynamics.

One of the disadvantages of using two steps to estimate the pilot model parameters is that the bias and variance of the non-parametric frequency responses can cause increased bias and variance in the obtained parameter estimates. A second disadvantage is that in order to estimate multiple frequency response functions in the first step, an equal number of forcing functions needs to be inserted into the closed-loop system to assure that the inputs to the pilot model are uncorrelated (see Figure 1).[8,11] Inserting multiple forcing functions may yield an unrealistic piloting task as compared to real flight and makes the data less comparable to classical single forcing function target-following and disturbance-rejection tasks used in many experiments described in literature.[6,7,10,26] When using Fourier coefficients or LTI models for estimating the frequency response functions, the forcing functions need to be carefully designed keeping in mind the requirements for identifiability of the frequency responses and the pilot limitations.[8]

II.D.2. Time-Domain Techniques

Time-domain parameter estimation techniques, such as the least-squares method and maximum likelihood estimation,[27] directly fit a parameter model on the time-domain data (see Figure 2). As time-domain signals generally have significantly more data points than the frequency response functions used in the frequency-domain methods, fitting the parameter model on the time-domain data requires more computational power. Another disadvantage is that it is difficult to determine the correct model structure beforehand and an incorrect model structure can not be easily detected by comparing the model output with the measured pilot output.

One of the advantages of a time-domain method is that the parameter model is directly fit using only one step, reducing the bias and variance of the estimated parameters compared to the frequency-domain methods. Also, there are fewer constraints when designing the forcing functions, as the frequency content of the signals has less influence on the identifiability of the parameters. There is also no explicit requirement for uncorrelated input signals of the pilot model as is the case using the frequency-domain methods.

In experiments, the differences in pilot control behavior for different experimental conditions are often small in magnitude. The increased accuracy of the estimated parameters for time-domain techniques could increase the significance of the results in these experiments. Also, as time-domain methods allow for more design freedom of the forcing functions, tasks which are more comparable to real piloting tasks can be used in experiments. This will increase the insight into multimodal perception and control for such tasks.

III. Genetic Maximum Likelihood Estimation

Maximum likelihood estimation (MLE) is a time-domain parameter estimation technique that has many applications.[19–23,28] One of the main reasons for this is that maximum likelihood estimates have some attractive statistical properties. They are consistent and efficient, which means that the parameter estimate converges to the true parameter set and that the variance reduces to the Cramér-Rao lower bound as the sample size increases.[29] Furthermore, the errors in the resulting parameter estimates have an unbiased Gaussian distribution.

In this section a procedure for estimating the parameters of multi-channel pilot models that is based on the principle of maximum likelihood will be described. The structure of such pilot models warrants the use of an output-error model structure, which results in a simplification of the full maximum likelihood estimation problem. To increase the probability of finding the global minimum of this nonlinear optimization problem, a genetic algorithm is used to determine the initial parameter estimates for a classical gradient-based parameter estimation procedure.

III.A. The Maximum Likelihood Method

The pilot model considered in this paper incorporates separate pilot visual and motion responses, as depicted in Figure 1. The pilot's control output u is considered to be the sum of a response to visual and motion cues (e and θ, respectively) and a remnant signal n.

Maximum likelihood estimation procedures generally require models that are written in state-space form. For the multi-channel pilot model of Figure 1, a discrete time state-space representation can be given by:

$$\begin{aligned} \dot{\bar{x}}(k+1) &= \begin{bmatrix} A_e(\Theta) & 0 \\ 0 & A_\theta(\Theta) \end{bmatrix} \bar{x}(k) + \begin{bmatrix} B_e(\Theta) & 0 \\ 0 & B_\theta(\Theta) \end{bmatrix} \begin{bmatrix} e(k) \\ \theta(k) \end{bmatrix} \\ u(k) &= \begin{bmatrix} C_e(\Theta) & -C_\theta(\Theta) \end{bmatrix} \bar{x}_s(k) + \begin{bmatrix} D_e(\Theta) & -D_\theta(\Theta) \end{bmatrix} \begin{bmatrix} e(k) \\ \theta(k) \end{bmatrix} + n(k). \end{aligned} \tag{9}$$

In Eq. (9), Θ represents the vector of unknown pilot model parameters as defined by Eq. (6). The subscripts e and θ divide the total state-space system into the state-space models of the error response function H_{pe} and the pitch response function $H_{p\theta}$, respectively. These state-space representations are easily obtained by converting the transfer function models defined in Equations (2) and (3) using the controller canonical form, as illustrated for $A_e(\Theta)$ by:

$$A_e(\Theta) = \begin{bmatrix} 0 & 1 & 0 & \cdots & 0 \\ 0 & 0 & 1 & \ddots & \vdots \\ \vdots & \ddots & \ddots & \ddots & 0 \\ 0 & 0 & \cdots & 0 & 1 \\ A_e(N_e,1) & A_e(N_e,2) & \cdots & A_e(N_e,N_e-1) & A_e(N_e,N_e) \end{bmatrix}, \tag{10}$$

where N_e is the order of $A_e(\Theta)$. For the conversion to a state-space representation, the pilot model time delays are approximated by using Padé approximations of typically fifth order, to ensure accurate description of the high-frequency phase roll-off. Especially due to these Padé approximations, the matrices of the state-space model as defined by Eq. (9) contain coefficients that are a highly nonlinear function of the pilot model parameters. For example, Equations (11) and (12) give the first and last coefficients in the final row of $A_e(\Theta)$ for a fifth order Padé approximation of the visual time delay τ_v.

$$A_e(N_e,1) = \frac{-30240\omega_{nm}^2}{T_{lag}\tau_v^5} \tag{11}$$

$$A_e(N_e,N_e) = \frac{-2T_{lag}\tau_v^5\zeta_{nm}\omega_{nm} - 30T_{lag}\tau_v^4 - \tau_v^5}{T_{lag}\tau_v^5} \tag{12}$$

The state-space pilot model given in Eq. (9) only has an additive noise term in the output equation, i.e., no process noise is assumed. This output-error structure significantly reduces the complexity of the MLE procedure. The pilot remnant n, which is accounted for by the measurement noise in the chosen model structure, is modeled as an additive zero-mean Gaussian white noise signal, whose properties are defined as:

$$E\{n(k)\} = 0;\ E\left\{n(k)\ n^T(k)\right\} = \sigma_n^2. \tag{13}$$

Maximum likelihood estimation techniques attempt to find an estimate $\hat{\Theta}$ of the parameter vector Θ that maximizes the likelihood function. The likelihood function $L(\Theta)$ is defined as the joint conditional probability density function of the prediction error for m measurements of $u(k)$:

$$L(\Theta) = f(\epsilon(1),\epsilon(2),\ldots,\epsilon(k),\ldots,\epsilon(m)|\Theta). \tag{14}$$

The prediction error, indicated as $\epsilon(k)$ in Eq. (14), is defined as the difference between the measured pilot control signal $u(k)$ and the modeled pilot control signal $\hat{u}(k)$ at discrete instants. Given the properties of the remnant as defined in Eq. (13), the conditional probability density function for one measurement of $\epsilon(k)$ is given by:

$$f(\epsilon(k)|\Theta) = \frac{1}{\sqrt{2\pi\sigma_n^2}} e^{-\frac{\epsilon^2(k)}{2\sigma_n^2}}. \tag{15}$$

The set of parameters that maximizes the likelihood function is the maximum likelihood estimate of the parameter vector Θ. For the MLE method it is common practice to minimize the negative natural logarithm of the likelihood function instead of maximizing $L(\Theta)$, as this results in a more straightforward optimization problem. When a global minimum of the negative log-likelihood is attained, the resulting parameter vector is the maximum likelihood estimate, indicated with $\hat{\Theta}_{ML}$. By combining Eq. (14) and Eq. (15) and considering the fact that the pilot model contains a single output, the following expression for this maximum likelihood estimate can be obtained:

$$\hat{\Theta}_{ML} = \arg\min_{\Theta} \; -\ln L(\Theta) = \arg\min_{\Theta} \left[\frac{m}{2} \ln \sigma_n^2 + \frac{1}{2\sigma_n^2} \sum_{k=1}^{m} \epsilon^2(k) \right]. \tag{16}$$

Eq. (16) summarizes the parameter estimation problem that is investigated for the estimation of multi-channel pilot model parameters in this paper. Similar to the frequency-domain methods, this is a highly nonlinear optimization problem, as described in Section II.D. To cope with this problem, a strategy is chosen here that uses a genetic algorithm to identify a solution close to the global minimum.

III.B. Genetic Likelihood Optimization

Genetic algorithms are commonly used to find approximate solutions to nonlinear optimization problems, and have been successful in many applications.[18,30] The problem solving capabilities of genetic algorithms are based on the principle of "survival of the fittest" as considered in evolutionary biology. In such an algorithm, a population of candidate solutions to the optimization problem is subjected to random genetic functions such as selection, mating, crossover and mutation. These functions cause the population to evolve toward increasingly better, i.e., more fit, solutions. The inherent randomness of genetic algorithms and the fact that a large number of different solutions are evaluated results in a high probability of finding the global minimum of an optimization problem.

Zaychik and Cardullo[18] used a genetic algorithm as the principal estimation procedure for identifying the parameters of the Hess operator model[5] from simulation data. However, in this research, maximum likelihood estimation was not used for the formulation of the optimization problem. Abutaleb[30] describes an application of a genetic algorithm to a maximum likelihood estimation problem. The negative logarithm of the likelihood function is used as the fitness criterion and the parameter sets that produce the lowest log-likelihood are defined to be the fittest members of the population.

In the maximum likelihood estimation method developed in this paper, a genetic algorithm is used to find sets of pilot model parameters that minimize the likelihood function defined by Eq. (14). At the start of a genetic optimization process a random population of parameter sets is generated within a lower and upper bound for all parameters. The fitness of all the members of the population is calculated. Next, iterations are performed with the following steps:

1. First, a random selection of members within the population is made. The members with the highest fitness will have the highest probability of being selected. The selected members will be used for mating.

2. The parameters of each member are coded into genes given their lower and upper

bound. A gene is a binary representation of the parameter value. For example, if the current value of a parameter is 1.6 and the lower bound and upper bound are respectively 0 and 2, a binary representation using 8 bits will be 11001100. The lower and upper bound will be 00000000 and 11111111, respectively. The higher the amount of bits used for the binary presentation, the higher the resolution of possible parameter values between the lower and upper bound.

3. For each parameter set two solutions are picked at random from the pool created in step 1. These two solutions will mate and produce offspring.

4. During the mating process, crossover between the genes will occur with a certain probability, usually set to 0.7. The crossover location is chosen randomly. For example, if we have two genes, 11001100 and 10101010, and a crossover location of 3, the two offspring will have genes given by 11001010 and 10101100.

5. Next, every bit in the genes of the offspring will mutate with a certain mutation probability. If a bit mutates, it changes from 0 to 1 or from 1 to 0. The mutation probability is typically very low, e.g., 0.01.

6. The offspring is decoded from binary codes into real values and their corresponding fitness is calculated.

7. A new population is chosen based on the fitness of the offspring and the original population.

The genetic optimization is terminated when a specified number of iterations of steps 1 to 7 has been performed.

Due to the limited gene size that is commonly selected for encoding of parameters in genetic algorithms to reduce the computational burden, the resulting parameter estimates tend to be relatively inaccurate. In addition, genetic algorithms are not deterministic and will give different results every time they are run. Therefore, a genetic algorithm is believed to be less suitable to be used as the sole estimation method for estimating pilot model parameters from measurement data.

III.C. Unconstrained Gauss-Newton Optimization

The parameter sets that are obtained from the genetic likelihood optimization have a high probability of being close to the global optimum of the optimization problem. To further refine these parameter estimates, the solutions of the genetic algorithm are used as the initial parameter estimates for an unconstrained Gauss-Newton optimization. This gradient-based

optimization method is the classical approach to solving maximum likelihood estimation problems.[23,29] The iterative parameter update equation for the Gauss-Newton optimization is given by:

$$\hat{\Theta}\,(i+1) = \hat{\Theta}\,(i) - \alpha\,(i)\,M_{\Theta\Theta}^{-1}(\hat{\Theta}\,(i))\frac{\partial L(\hat{\Theta}\,(i))}{\partial \Theta}. \tag{17}$$

The gradients of the likelihood function with respect to all parameters, $\partial L/\partial\Theta$, can be evaluated using the Jacobians of all state-space matrices with respect to the parameter vector Θ. The Fisher information matrix, indicated with the symbol $M_{\Theta\Theta}$ in Eq. (17), is given by:

$$M_{\Theta\Theta} = \frac{1}{\sigma_n^2}\sum_{k=1}^{m}\left(\frac{\partial \epsilon(k)}{\partial \Theta}\right)^2. \tag{18}$$

The Fisher information matrix is symmetrical and should be positive definite, i.e., full rank, as it needs to be inverted for the parameter update (Eq. (17)). The inverse of the Fisher information matrix yields the Cramér-Rao lower bound (CRLB), i.e., the minimum achievable variance of the parameter estimate. Both the Fisher information matrix and the first-order gradient of the likelihood function vary with the magnitude of the estimation error ϵ, yielding parameter update steps of larger magnitude if estimation errors are larger. In some instances, this causes the Gauss-Newton optimization to become unstable if initial parameter errors are large: in that case the first parameter update may force the unconstrained algorithm to a region of meaningless and inaccurate solutions from which it cannot recover.

Using the solution of a genetic algorithm as proposed here as the initial parameter estimate for the Gauss-Newton optimization reduces the occurrence of such undesired effects significantly. A second measure that can be taken to avoid this behavior is by considering the line-search parameter α in Eq. (17). This parameter, which typically varies between 0 and 1, is determined at each iteration before the actual parameter update to ensure optimal (i.e., most rapid) minimization of the likelihood function. This is illustrated in Figure 3, where a typical variation of the likelihood L is depicted as a function of α. For the example shown in Figure 3 it is clear that $\alpha = 0.8$ yields a superior parameter set after the update step than would be obtained for $\alpha = 1$.

The resolution that is considered for α during the optimization – indicated with circles in Figure 3 – can be selected freely and is highly dependent on the application. For the pilot model estimation problem considered here, it was found that for the first iterations a rather coarse spacing of α, i.e. 0.1, already yielded enough added stability to the optimization algorithm. When parameter estimates came closer to their optimal values, it was found that small improvements could still be made for very small values of α. Therefore, a finer spacing of α, i.e. 0.01, was considered below 0.2 (see Figure 3).

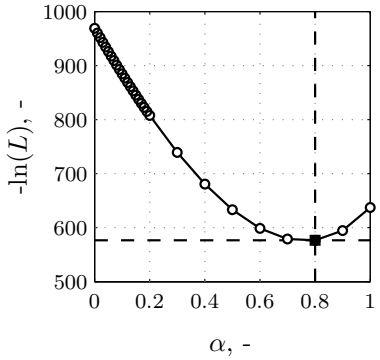

Figure 3. Typical likelihood variation along search vector.

IV. Results

In this section, the genetic maximum likelihood method will be evaluated using experimental data. In addition, the parameter estimation results from the experimental data will be used in multiple pilot model simulations with increasing remnant levels to investigate the robustness of the method to increasing pilot remnant (measurement noise).

IV.A. Application to Experiment Data

The experiment was performed in the SIMONA Research Simulator of the Delft University of Technology, Faculty of Aerospace Engineering. The objective of the experiment was to investigate the effects of pitch rotational motion and heave motion on multimodal pilot control behavior in an aircraft pitch control task. The experiment had a full factorial design with eight conditions with varying motion cues. In every condition, pitch rotational motion and two distinct components of heave motion could be either on or off.

The genetic maximum likelihood method was used to estimate the parameters of the pilot model using the experimental data. In this section, the performance results of the genetic MLE method will be given for data of one subject for one of the experimental conditions. In this condition, rotational pitch motion was available in addition to the cues from a compensatory display. The subject for which the performance data is shown was chosen randomly.

IV.A.1. Experimental Measurements

Seven subjects participated in the experiment. All had experience with similar manual control tasks from previous human-in-the-loop experiments. Two subjects have additional experience as aircraft pilots. The subjects ages ranged from 25 to 46 years old. Before starting the experiment, the subjects received an extensive briefing on the scope and objective

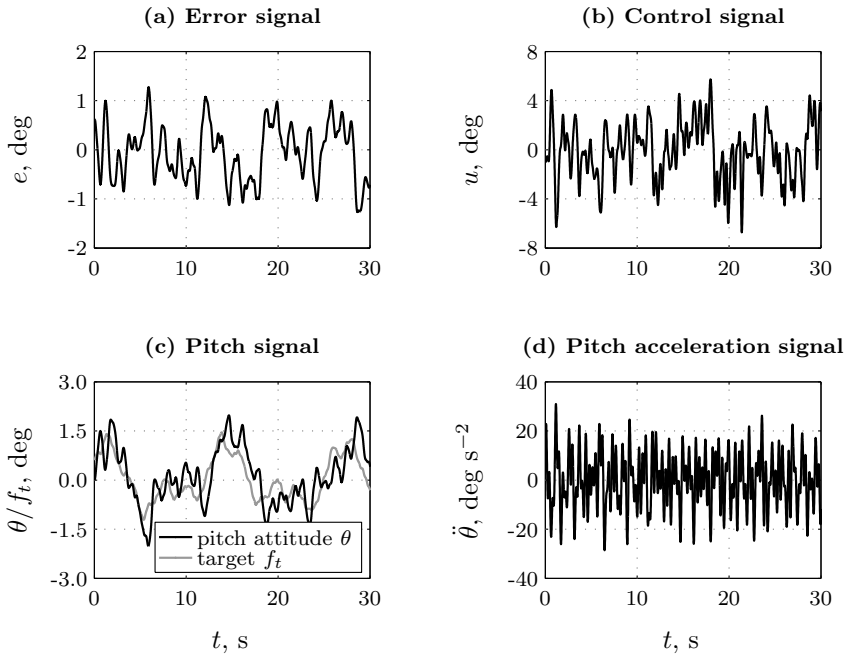

Figure 4. Average time traces of various loop signals (subject 1).

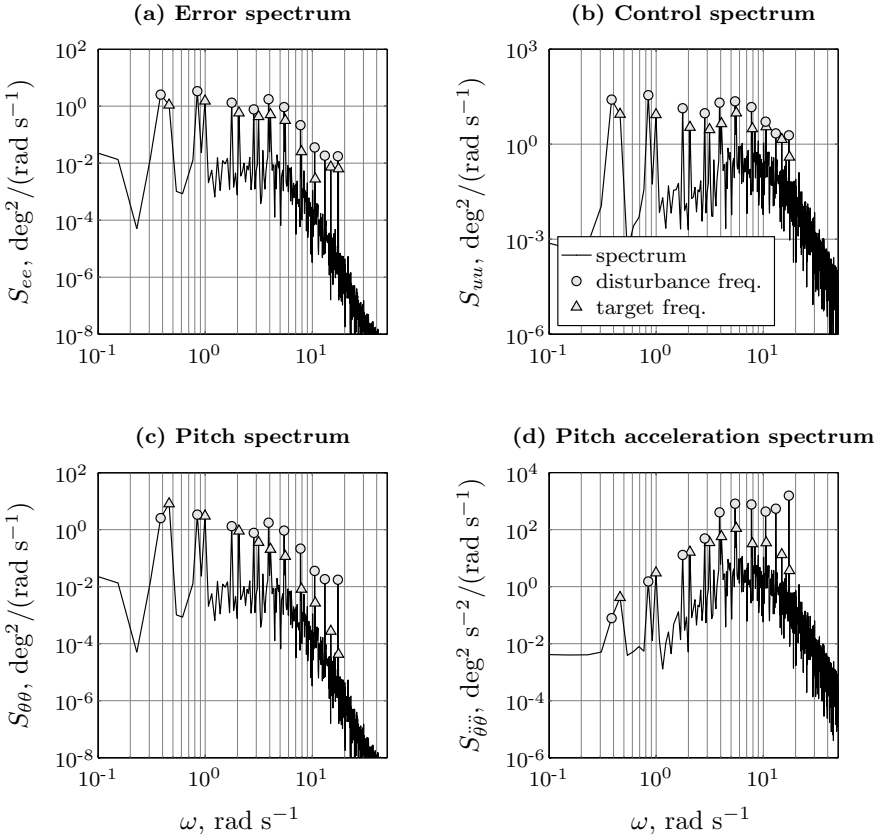

Figure 5. Average loop signal spectra (subject 1).

of the experiment. The main instruction they received before the experiment was to attempt to minimize the pitch tracking error, i.e., the signal that was presented on the visual display, as best as possible.

The experiment started with a considerable number of training runs. The training phase ended when a constant level of performance was achieved. After the training phase, 5 repetitions of every condition were performed in a random order, of which the data was used in the final results. Each individual experiment run lasted 110 seconds, of which the last 81.92 seconds were used as the measurement data. Participants generally need some time to stabilize the disturbed aircraft model after the start of a run, therefore the data from the first 28.08 seconds of each run were discarded. Data was logged at a frequency of 100 Hz. Further details of the experiment setup can be found in Reference 2.

Time traces of all signals depicted in Figure 1 were recorded during the experiment. To reduce the noise content in the signals and improve pilot model parameter estimates, the time traces of the five repetitions performed by each subject were averaged for the identification procedure.[8] Examples of averaged time traces of the error signal e, the control signal u, the pitch attitude θ and pitch acceleration $\ddot{\theta}$ are depicted in Figure 4. The time trace of the pitch target signal f_t is shown alongside that of the pitch attitude for reference.

Note from Figure 4 that the subjects successfully made the aircraft pitch attitude follow the target signal f_t. Most of the additional oscillations in pitch attitude can be attributed to the presence of the disturbance signal.

The power spectral densities of the time traces given in Figure 4 are given in Figure 5. The input frequencies of the forcing functions, as given in Table 1, are indicated with circles and triangles for f_d and f_t, respectively. The signal-to-noise ratio at the input frequencies is high for all the signals in the control loop.

IV.A.2. Algorithm Performance

The error, pitch acceleration and control signals given in Figure 4 are used to estimate the pilot model parameters with the genetic maximum likelihood method. Before the Gauss-Newton optimization, 100 iterations with the genetic algorithm are performed. The parameter lower bounds were set to zero and the upper bounds were taken positive and large enough to account for all relevant solutions of the estimation problem (see Table 2). For the parameter conversion to binary strings, 20 bits are used. Values for the crossover and mutation probabilities were set to 0.7 and 0.01, respectively. The solution of the Genetic algorithm is used as the initial parameter set for the Gauss-Newton optimization. The Gauss-Newton optimization is terminated if the derivative of the parameters with respect to the search vector is smaller than 10^{-6}.

Typically, 100 repetitions of the algorithm are performed on a single data set, of which

Table 2. Lower and upper parameter bounds used in the genetic algorithm.

	K_v	T_{lead}	T_{lag}	K_m	τ_v	τ_m	ω_{nm}	ζ_{nm}
	-	s	s	-	s	s	rad s^{-1}	-
lower bound	0.0	0.0	0.0	0.0	0.0	0.0	5.0	0.0
upper bound	5.0	10.0	10.0	10.0	1.0	1.0	20.0	1.0

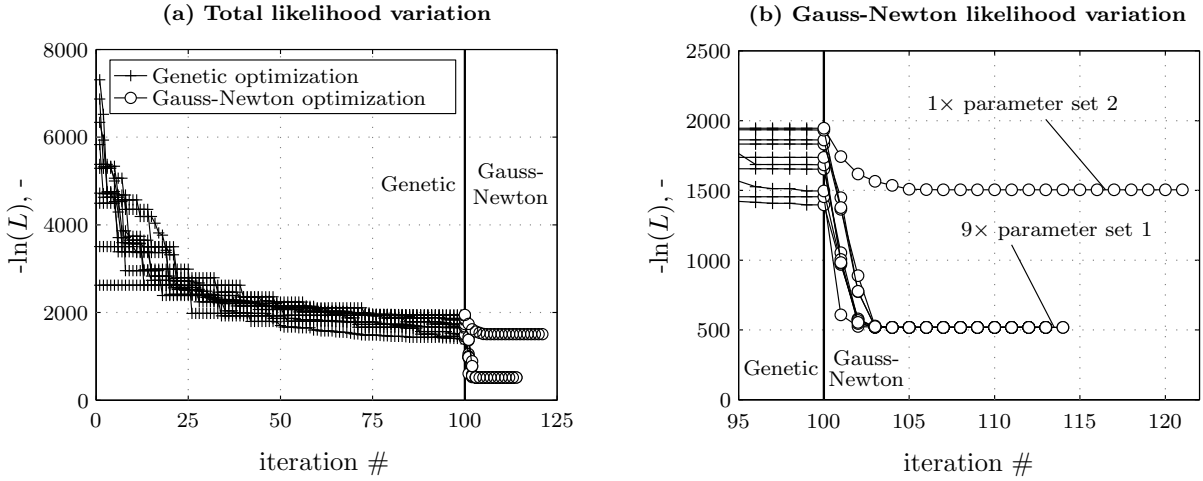

Figure 6. Changes in negative logarithm of the likelihood during optimization (10 repetitions, subject 1).

the ten with the lowest likelihood are further evaluated using Gauss-Newton optimization. The negative logarithm of the likelihood for these ten repetitions is given in Figure 6. It is clear from Figure 6b that the solution of the genetic algorithm is different for all repetitions. After refinement by the Gauss-Newton algorithm, two different sets of parameters are found. The solution with the lowest negative logarithm of the likelihood is found nine times. In one instance, the optimization ends up in a different (local) minimum, which clearly has a higher likelihood.

This illustrates the nonlinearity of the optimization problem. For data from other subjects, none to up to three of the obtained parameter sets were found to represent local minima. Note that a local minimum was never attained more often than the global minimum.

To illustrate the significance of this result, pilot model parameters were also estimated by using only the Gauss-Newton maximum likelihood algorithm. To illustrate the large influence of the initial parameter estimate on the results of this gradient-based optimization, a large number of initial conditions were evaluated. For all parameters, a number of different values were selected between the upper and lower bounds defined for the genetic algorithm. The full factorial of all these initial parameter values yielded 40000 different initial parameter sets. Figure 7 depicts the likelihood of the final parameter estimates obtained with the Gauss-Newton algorithm for all these different initial estimates, in ascending order.

The leftmost shaded area in Figure 7 indicates the set of initial conditions for which the

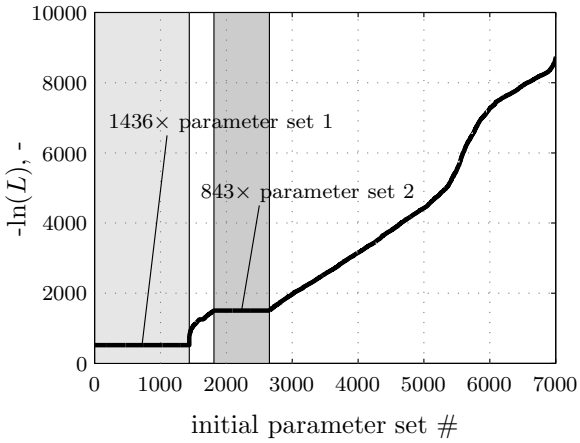

Figure 7. Negative log-likelihood of Gauss-Newton parameter estimates for 7000 different initial parameter sets, sorted in ascending order (subject 1).

Gauss-Newton algorithm attained parameter estimate 1, as depicted in Figure 6; the second shaded area, which corresponds to a solution with a higher likelihood, are the occurrences for which parameter set 2 was found. All parameter sets that are outside either of the shaded areas in Figure 7 represent initial estimates for which the algorithm was unable to converge. Note that the Gauss-Newton algorithm only converged to the global minimum (parameter set 1) for around 20% of all tested initial conditions. For all other initial conditions, the Gauss-Newton parameter estimation procedure would either converge to an incorrect minimum, or fail to converge to a stable solution. As illustrated by Figure 6, the addition of the genetic algorithm ensures reliable estimation of the parameter set that represents the global minimum.

IV.A.3. Pilot Describing Functions

Figure 8 gives the linear pilot response functions H_{pe} and $H_{p\theta}$ for the two different solutions found by the algorithm depicted in Figure 6b. The Fourier coefficients, which can be analytically calculated from the measured time-domain data, coincide with parameter set 1. This is a further indication that parameter set 1 represents the correct solution of the parameter estimation problem. The parameter values and the square root of the diagonal of the CRLB resulting from the Gauss-Newton optimization are given in Table 3. Note that the CRLB is found to be higher for nearly all parameter estimates of parameter set 2. From the parameter values, it can be seen that the gain for the vestibular channel K_m is much higher for parameter set 1. In parameter set 2 the lower gain for the vestibular channel is compensated for by the higher values for the lead and lag time constants. The vestibular time delay is higher than the visual time delay for parameter set 2, which disagrees with findings from previous research.[2,6,7] Finally, the neuromuscular frequency found for parameter set 1 is

higher than that obtained for parameter set 2.

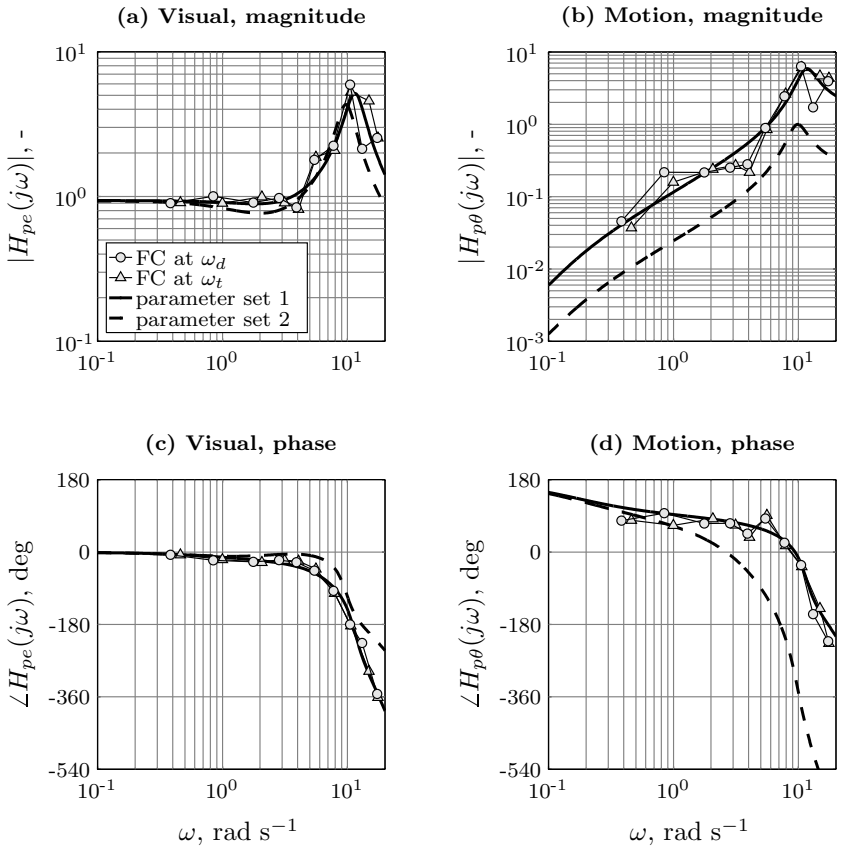

Figure 8. Bode plot of the pilot visual and motion response for parameter sets 1 and 2 (subject 1).

Table 3. Values and standard deviation for parameter sets 1 and 2 (subject 1).

parameter	parameter set 1		parameter set 2	
	$\hat{\Theta}$	$\sqrt{\text{CRLB}(\hat{\Theta})}$	$\hat{\Theta}$	$\sqrt{\text{CRLB}(\hat{\Theta})}$
K_v, -	0.938	$6.77{\cdot}10^{-3}$	0.932	$8.91{\cdot}10^{-3}$
T_{lead}, s	0.278	$6.47{\cdot}10^{-3}$	0.337	$9.21{\cdot}10^{-3}$
T_{lag}, s	0.502	$1.92{\cdot}10^{-2}$	0.774	$3.08{\cdot}10^{-2}$
K_m, -	0.692	$1.29{\cdot}10^{-2}$	0.147	$1.11{\cdot}10^{-2}$
τ_v, s	0.268	$2.79{\cdot}10^{-3}$	0.134	$2.41{\cdot}10^{-3}$
τ_m, s	0.175	$1.94{\cdot}10^{-3}$	0.679	$1.29{\cdot}10^{-2}$
ω_{nm}, rad s^{-1}	11.560	$6.41{\cdot}10^{-2}$	9.775	$7.15{\cdot}10^{-2}$
ζ_{nm}, -	0.175	$4.60{\cdot}10^{-3}$	0.168	$9.56{\cdot}10^{-3}$

The measured pilot control signal is compared with the model output for the two parameter solutions in Figure 9. It can be seen that the difference between both solutions in the time domain is only very small. The variance accounted for (VAF), which is a measure of the correlation of two time-domain signals,[8] is only marginally higher for parameter set 1.

Figure 10 gives the pilot frequency response functions corresponding to the optimal parameter estimate for all subjects for the experimental condition used in this paper. From

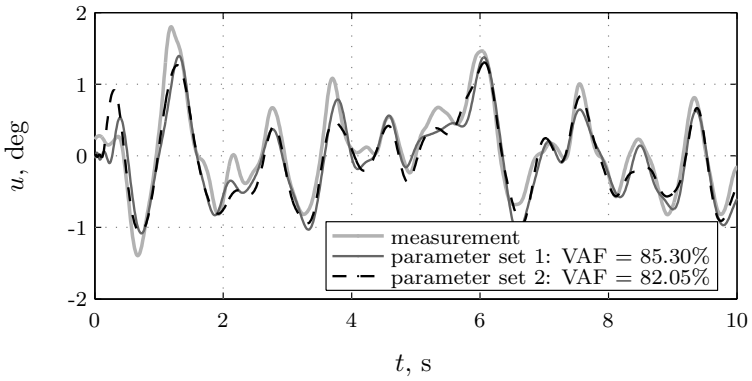

Figure 9. Comparison of model control signals for parameter sets 1 and 2 (subject 1).

this figure it can be seen that all subjects give consistent results. The response functions vary slightly between subjects as every individual has a different control strategy, which is commonly seen in this type of experiments.

IV.A.4. Pilot Remnant

The pilot remnant is determined by the difference between the model output of the linear pilot model and the measured pilot control signal, as depicted in Figure 9. A time trace of the pilot remnant for the model with parameter set 1 is given in Figure 11a. The power spectrum of this signal is given in Figure 11b. It can be seen that the spectrum has the approximate characteristics of a third-order low-pass filter with a damping coefficient:

$$H_n(j\omega) = \frac{K_n\ \omega_n^3}{((j\omega)^2 + 2\zeta_n\omega_n j\omega + \omega_n^2)\,(j\omega + \omega_n)}, \tag{19}$$

with $K_n = 2.6$ the remnant intensity and $\zeta_n = 0.26$ and $\omega_n = 12.7$ rad/s the remnant filter damping factor and break frequency, respectively. Similar characteristics are found in previous research.[8]

The probability density function of the pilot remnant is given in Figure 12. This figure clearly shows that the remnant signal has a distribution that is almost perfectly Gaussian with a zero mean, as is assumed in Eq. (13). The low-pass remnant spectrum has no effect on the normality of the signal. The fact that the remnant is distinctly non-white, as shown in Figure 11b, may cause extra bias in the pilot model parameter estimates, which has been further investigated using off-line simulations.

IV.B. Off-line Simulations

To investigate the robustness of the genetic MLE method to increasing levels of pilot remnant, parameter set 1 is used to perform multiple simulations of the closed-loop control task with

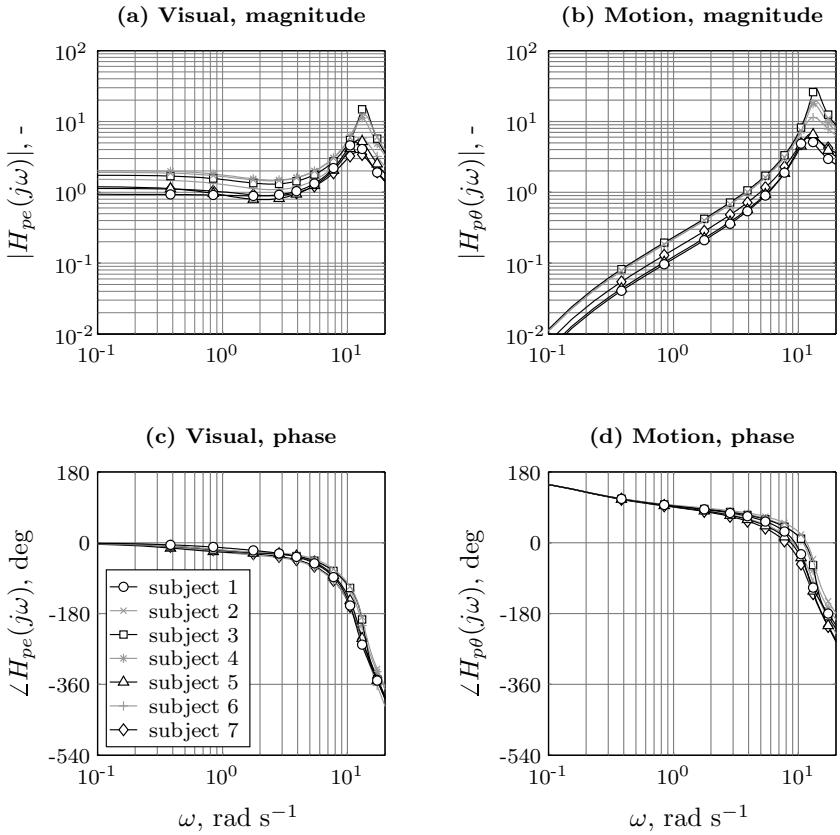

Figure 10. Bode plot of the pilot visual and motion response for all experiment subjects.

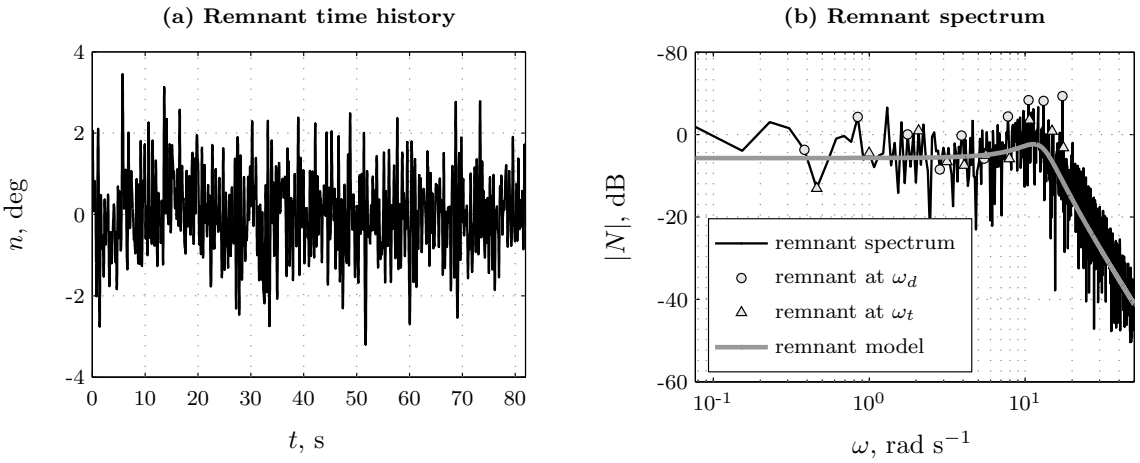

Figure 11. Pilot remnant characteristics (subject 1).

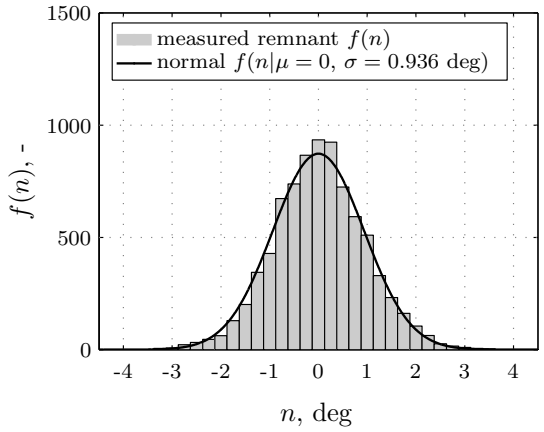

Figure 12. Remnant probability density function (subject 1).

increasing levels of remnant. The remnant filter break frequency ω_n and damping factor ζ_n are kept constant and the remnant intensity K_n is gradually increased to achieve the desired ratio between control signal power and remnant power. The ratio is increased from 0 to 0.5, while the value found for the averaged experimental data is approximately 0.15 for parameter set 1. For each remnant level, eighty simulations are performed, each with a different noise realization.

Figure 13 shows the average parameter bias found by applying the genetic MLE procedure to the data of each simulation. Also, the 99% confidence interval for each parameter is indicated in this figure. It can be seen that for increasing levels of pilot remnant, the average bias of the parameter estimates increases. For all parameters, the average bias remains within the 99% confidence interval, which indicates that the bias is not significant. At a remnant-control signal power ratio of 0.15, found experimentally, the bias is relatively small for all parameters.

V. Discussion

This paper presents a new strategy for the estimation of multi-channel pilot model parameters from time-domain data based on maximum likelihood estimation. The classical MLE method, with only a gradient-based algorithm to estimate the parameters, is very dependent on the initial parameter guess. This is highly undesirable given the fact that the cost function is highly nonlinear and contains many local minima. For this reason, a genetic algorithm was used in combination with the gradient-based Gauss-Newton optimization procedure. The genetic algorithm does not require an initial parameter guess and is far less sensitive to local minima, as a population of possible solutions is kept until the algorithm terminates. The subsequent use of a Gauss-Newton algorithm increases the accuracy of the parameter estimate, as gradient information is included. The method was successfully

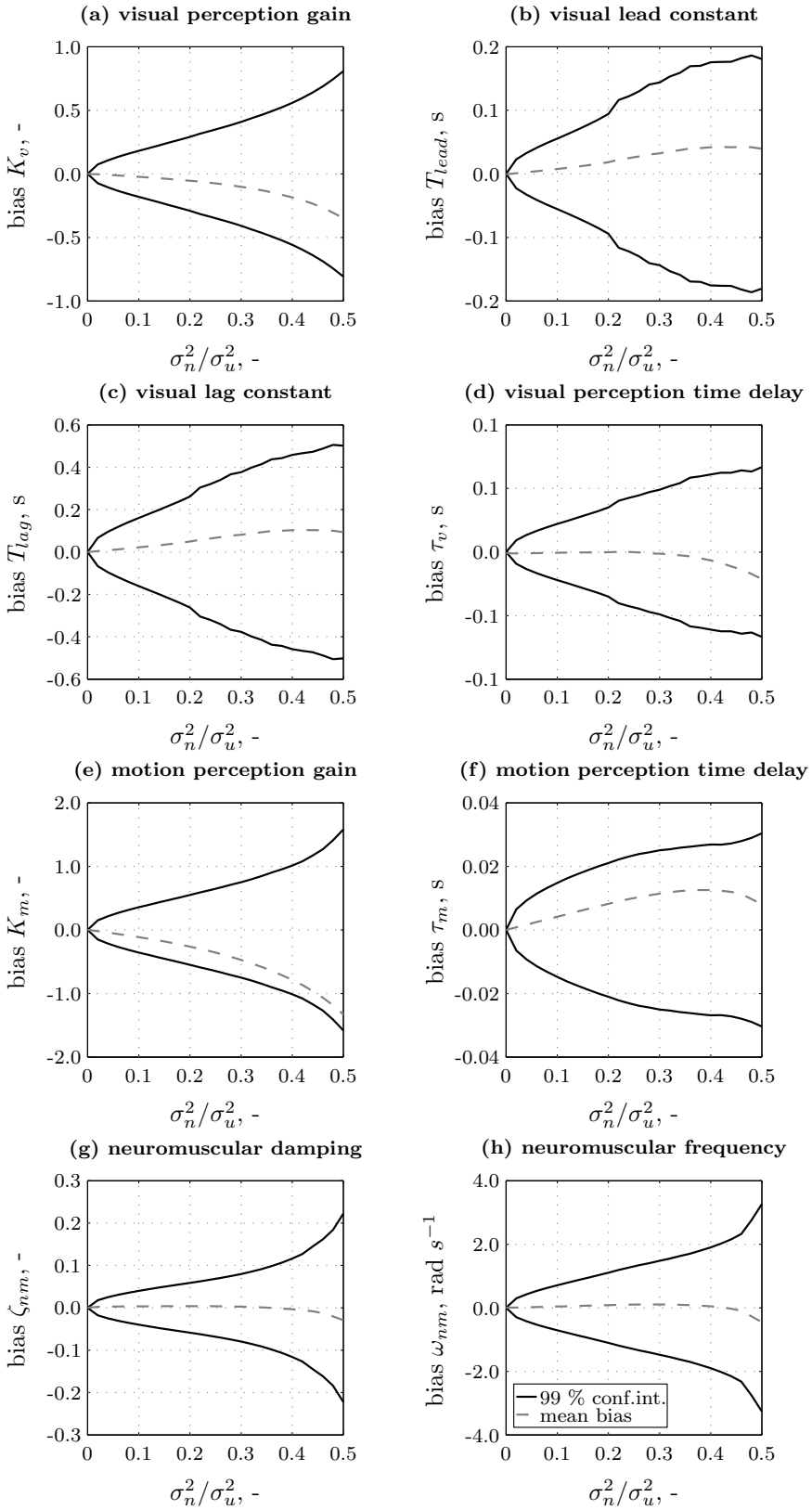

Figure 13. Average parameter bias for different remnant levels.

applied to data from an experiment investigating the influence of pitch and heave motion cues on pilot control behavior.

Applying the genetic maximum likelihood algorithm to the experiment data multiple times for all subjects resulted in the occurrence of solutions other than the global optimum. These occurrences were infrequent, however, and the corresponding solutions always have a higher likelihood than the global minimum. Hence, the optimization should be performed several times for each condition from an experiment to ensure that the global optimum solution is found. The often subtle differences between the parameter sets of a local or a global optimum, and the equivalence of the resulting time-domain fits make it difficult to distinguish between these solutions based on this information alone. Although, Fourier coefficients can provide an indication of the frequency response of the global optimum, these can only be computed when multi-sine signals are used as forcing functions.

Simulations have been performed to investigate the robustness of the MLE method to increasing levels of remnant. It was found that the average bias of the parameters increases for increasing levels of remnant power. The bias remained within the 99% confidence interval of the parameter estimate, which indicates that the bias is not significant. For the parameter estimation on averaged time-domain data of five runs ($\sigma_n^2/\sigma_u^2 \approx 0.15$) the bias of the parameter estimates is relatively small. When individual runs ($\sigma_n^2/\sigma_u^2 \approx 0.30$) are used in the parameter estimation procedure, the bias becomes more substantial, however.

As maximum likelihood estimates have the property to be unbiased for infinite measurement times, the increase in bias for higher levels of remnant is an unexpected result. Although this bias is partly caused by the finite measurement times, the fact that the remnant is colored rather than purely Gaussian white noise may cause an additional bias. Also, because of a correlation between the pilot model input and output in the closed loop – the remnant, which is part of the output of the pilot model, travels around and is also present in the input of the pilot model – an additional bias may be present. A solution for both problems would involve inclusion of process noise into the state-space representation of the pilot model, which requires a prediction-error algorithm to be added to the MLE method. This allows for the properties of the remnant filter to be estimated, and could reduce the bias in the parameter estimates at higher levels of remnant. The Kalman filter that is needed to solve this problem, however, will increase the complexity of the parameter estimation procedure and will significantly increase the computational burden.

In this paper, the genetic MLE method is evaluated with data from an experiment where multi-sine signals were used as forcing functions. Parameter estimation in the time domain also allows the use of novel types of input signals, however, such as ramp or step signals that are often considered in other system identification problems. These signals can be used as target signal and may yield a control task that is much more similar to real piloting tasks. An

investigation on the use of these signals is already performed,[24] but more research is needed to evaluate the performance of the MLE method with these signals. The maximum likelihood parameter estimation algorithm can also be used to identify multi-channel pilot models when only *one* forcing function is present, as long as all the inputs to the pilot model are sufficiently excited. The method has already been successfully applied to measurement data from human-in-the-loop experiments where pure target-following tasks were considered.[31,32]

Finally, the use of a genetic algorithm allows for the introduction of nonlinear elements into the pilot model, as no gradient information is required. An example can be the addition of motion perception thresholds. This will also be a subject of future research.

VI. Conclusions

A pilot model parameter estimation technique, based on the maximum likelihood method, was introduced and enhanced with a genetic algorithm to considerably improve performance. The new method was successfully applied to data from an experiment investigating the role of pitch and heave motion during pitch control of an aircraft. The parameters of the multi-channel pilot model and the properties of the remnant could be accurately estimated from the time-domain signals. Using multiple iterations of the algorithm on a single data set, the global optimum solution was found for 90% of the cases. Using multiple simulations with different levels of pilot remnant, it was shown that there is no significant bias in the parameters for lower remnant levels. For high levels of pilot remnant bias is more substantial, caused by the fact that remnant tends to be colored rather than purely white noise.

Acknowledgments

This research was supported by the Technology Foundation STW, the applied science division of NWO, and the technology program of the Ministry of Economic Affairs. The authors would like to thank Tom Berger, currently affiliated with the NASA Ames Research Center, for his initial investigation into maximum likelihood estimation of pilot model parameters.

References

[1]Hosman, R. J. A. W., "Are Criteria for Motion Cueing and Time Delays Possible?" *Proceedings of the AIAA Modelling and Simulation Technologies Conference and Exhibit, Portland (OR)*, No. AIAA-1999-4028, 1999.

[2]Zaal, P. M. T., Pool, D. M., De Bruin, J., Mulder, M., and Van Paassen, M. M., "Use of Pitch and Heave Motion Cues in a Pitch Control Task," *Journal of Guidance, Control and Dynamics*, Accepted for

publication, November 2008.

[3]Stapleford, R. L., McRuer, D. T., and Magdaleno, R., "Pilot Describing Function Measurements in a Multiloop Task," *IEEE Transactions on Human Factors in Electronics*, Vol. HFE-8, No. 2, 1967, pp. 113–125.

[4]Stapleford, R. L., Peters, R. A., and Alex, F. R., "Experiments and a Model for Pilot Dynamics with Visual and Motion Inputs," Tech. Rep. NASA CR-1325, NASA, 1969.

[5]Hess, R. A., "Model for Human Use of Motion Cues in Vehicular Control," *Journal of Guidance, Control, and Dynamics*, Vol. 13, No. 3, 1990, pp. 476–482.

[6]Van der Vaart, J. C., *Modelling of Perception and Action in Compensatory Manual Control Tasks*, Doctoral dissertation, Faculty of Aerospace Engineering, Delft University of Technology, 1992.

[7]Hosman, R. J. A. W., *Pilot's Perception and Control of Aircraft Motions*, Doctoral dissertation, Faculty of Aerospace Engineering, Delft University of Technology, 1996.

[8]Nieuwenhuizen, F. M., Zaal, P. M. T., Mulder, M., van Paassen, M. M., and Mulder, J. A., "Modeling Human Multichannel Perception and Control Using Linear Time-Invariant Models," *Journal of Guidance, Control, and Dynamics*, Vol. 31, No. 4, July–Aug. 2008, pp. 999–1013.

[9]Ellerbroek, J., Stroosma, O., Mulder, M., and van Paassen, M. M., "Role Identification of Yaw and Sway Motion in Helicopter Yaw Control Tasks," *Journal of Aircraft*, Vol. 45, No. 4, July–Aug. 2008, pp. 1275–1289.

[10]McRuer, D. T. and Jex, H. R., "A Review of Quasi-Linear Pilot Models," *IEEE Transactions on Human Factors in Electronics*, Vol. HFE-8, No. 3, 1967, pp. 231–249.

[11]Van Paassen, M. M. and Mulder, M., "Identification of Human Operator Control Behaviour in Multiple-Loop Tracking Tasks," *Proceedings of the Seventh IFAC/IFIP/IFORS/IEA Symposium on Analysis, Design and Evaluation of Man-Machine Systems, Kyoto Japan*, Pergamon, Kidlington, Sept. 16–18 1998, pp. 515–520.

[12]Stepner, D. E. and Mehra, R. K., "Maximum Likelihood Identification and Optimal Input Design for Identifying Aircraft Stability and Control Derivatives," Tech. Rep. NASA CR-2200, National Aeronautics and Space Administration, Washington, D. C., 1973.

[13]Taylor, L. W., "A Comparison of Human Response Modeling in the Time and Frequency Domains," *Third Annual NASA-University Conference on Manual Control*, 1967, pp. 137–156.

[14]Shirley, R. S., "A Comparison of Techniques for Measuring Human Operator Frequency Response," *Proceedings of the Sixth Annual Conference on Manual Control*, 1970, pp. 803–870.

[15]Phatak, A. V., R. K. Mehra, R., and Day, C., "Application of System Identification to Modeling the Human Controller under Stress Conditions," *IEEE Transactions on Automatic Control*, Vol. 20, No. 5, October 1975, pp. 657 – 664.

[16]Ninz, N. R., "Parametric Identification of Human Operator Models," *Proceedings of the Sixteenth Annual Conference on Manual Control*, 1980, pp. 137–145.

[17]Schmidt, D. K., "Time Domain Identification of Pilot Dynamics and Control Strategy," *Eighteenth Annual Conference on Manual Control*, 1982, pp. 19–40.

[18]Zaychik, K. B. and Cardullo, F. M., "Genetic Algorithm Based Approach for Parameters Estimation of the Hess Operator Model," *Proceedings of the AIAA Modeling and Simulation Technologies Conference and Exhibit, Hilton Head (SC)*, No. AIAA-2007-6893, 2007.

[19]Maine, R. and Iliff, K., "AGARD Flight Test Techniques Series Volume 3 on Identification of Dynamic Systems – Applications to Aircraft Part 1: The Output Error Approach," AGARDograph No. 300 AGARD-AG-300-VOL.3 PART I, North Atlantic Treaty Organization (NATO), 1986.

[20]Chu, Q. P., Mulder, J. A., and van Woerkom, P. T. L. M., "Modified Recursive Maximum Likelihood Adaptive Filter for Nonlinear Aircraft Flight-Path Reconstruction," *Journal of Guidance, Control, and Dynamics*, Vol. 19, No. 6, Nov.–Dec. 1996, pp. 1285–1295.

[21]Milne, G., Mulder, J. A., Soijer, M. W., Juliana, S., and Hermansyah, "Maximum Likelihood Stability & Control Derivative Identification of a Cessna Citation II," *Proceedings of the AIAA Atmospheric Flight Mechanics Conference and Exhibit, Montreal (Ca)*, No. AIAA-2001-4013, 2001.

[22]Mehra, R. K. and Prasanth, R. K., "Time-Domain System Identification Methods for Aeromechanical and Aircraft Structural Modeling," *Journal of Aircraft*, Vol. 41, No. 4, July-August 2004, pp. 721–729.

[23]Chu, Q. P., *Maximum Likelihood Parameter Identification of Flexible Spacecraft*, Ph.D. thesis, Delft University of Technology, 1987.

[24]Zaal, P. M. T., Pool, D. M., Mulder, M., and van Paassen, M. M., "New Types of Target Inputs for Multi-Modal Pilot Model Identification," *Proceedings of the AIAA Modeling and Simulation Technologies Conference and Exhibit, Honolulu (HI)*, No. AIAA-2008-7106, 18–21 Aug. 2008.

[25]Löhner, C., Mulder, M., and van Paassen, M. M., "Multi-Loop Identification of Pilot Central Visual and Vestibular Motion Perception Processes," *Proceedings of the AIAA Modeling and Simulation Technologies Conference and Exhibit, San Francisco (CA)*, No. AIAA-2005-6503, 15–18 Aug. 2005.

[26]Pool, D. M., Mulder, M., van Paassen, M. M., and van der Vaart, J. C., "Effects of Peripheral Visual and Physical Motion Cues in Roll-Axis Tracking Tasks," *Journal of Guidance, Control, and Dynamics*, Vol. 31, No. 6, 2008, pp. 1608–1622.

[27]Ljung, L., *System Identification Theory for the User*, Prentice Hall, Inc., 2nd ed., 1999.

[28]Berger, T., Zaal, P. M. T., Mulder, M., and van Paassen, M. M., "Time Domain Pilot Model Identification Using Maximum Likelihood Estimation," *Proceedings of the AIAA Modeling and Simulation Technologies Conference and Exhibit, Honolulu (HI)*, No. AIAA-2008-7109, 18–21 Aug. 2008.

[29]Mulder, J. A., *Design and Evaluation of Dynamic Flight Test Manoeuvres*, Ph.D. thesis, Delft University of Technology, 1986.

[30]Abutaleb, A. S., "A Genetic Algorithm for the Maximum Likelihood Estimation of the Parameters of Sinusoids in a Noisy Environment," *Circuits Systems Signal Processing*, Vol. 16, No. 1, 1997, pp. 69–81.

[31]Pool, D. M., Zaal, P. M. T., Mulder, M., van Paassen, M. M., and Mulder, J. A., "Parameter Estimation of Multimodal Pilot Models for Manual Target-following Tasks," *Proceedings of the 27th European Annual Conference on Human Decision-Making and Manual Control*, June 12–13 2008.

[32]Zaal, P. M. T., Mulder, M., van Paassen, M. M., and Mulder, J. A., "Maximum Likelihood Estimation of Multi-Modal Pilot Control Behavior in a Target-Following Task," *Proceedings of the IEEE International Conference on Systems, Man and Cybernetics, 2008.*, Oct. 12–15 2008.